Final Technical Report for NASA Graduate Student Researchers Program Award No. NGT 51038

Development of Silicon Microstructures for X-Ray Optics

Prepared by

Andrew Chen, Graduate Research Assistant, Columbia University

Philip Kaaret, Assosciate Professor of Physics, Columbia University.

Linda Miller, Group Leader, Jet Propulsion Laboratory

1 Summary

The goal of this research program was to develop a novel technique for focusing x-rays based on the optical system of a lobster's eye. A lobster eye employs many closely packed reflecting surfaces arranged within a spherical or cylindrical shell. These optics have two unique properties: they have unlimited fields of view and can be manufactured via replication of identical structures. Because the angular resolution is given by the ratio of the size of the individual optical elements to the focal length, optical elements with sizes on the order of one hundred microns are required to achieve good angular resolution with a compact telescope.

We employed anisotropic etching of single crystal silicon wafers for the fabrication of micron-scale optical elements. This technique, commonly referred to as silicon micromachining, is based on silicon fabrication techniques developed by the microelectronics industry. An anisotropic etchant is a chemical which etches certain silicon crystal planes much more rapidly than others. Using wafers in which the slowly etched crystal planes are aligned perpendicular to the wafer surface, it is possible to etch a pattern completely through a wafer with very little distortion. Our optics consist of rectangular pores etched completely through <110> oriented silicon wafers. The larger surfaces of the pores (the mirror elements) were aligned with the <111> planes of the crystal perpendicular to the wafer surface. The first silicon microfabrication was performed by Dr. Thomas Kenny at the Jet Propulsion Laboratory in the spring of 1992. Mr. Chen visited JPL for the summers of 1992, 1993, and 1994 during which time most of the silicon fabrication was performed.

We have succeeded in producing silicon lenses with a geometry suitable for 1-d focusing x-ray optics (Chen 1993, 1994). These lenses have an aspect ratio (40:1) suitable for x-ray reflection and have very good optical surface alignment. We have developed a number of process refinements which improved the quality of the lens geometry and the repeatability of the etch process. A significant progress was made in obtaining good optical surface quality. The RMS roughness was decreased from 110 Å for our initial lenses to 30 Å in the final lenses. A further factor of three improvement in surface quality is required for the production of efficient x-ray optics. In addition to the silicon fabrication, an x-ray beam line was constructed at Columbia for testing the optics. In addition to the individuals listed on the cover page, three students from Columbia were involved in this work: Eric Ford, a graduate student, and Jay Demas and Nashrid Kibria, both undergraduates.

2 Lobster Eye Optics

The novel optical devices for x-ray astronomy that we are developing are based on the lobster's optical system (Land 1972). A lobster eye lens is a spherical shell made of many channels with square cross sections; the cross section of such a lens is shown in Figure 1. The sides of the tubes are reflective and point toward the center of curvature of the shell. Parallel light rays from a distant object are focused by external reflection onto a focal surface with a radius of curvature equal to half that of the shell. Since the lens has no intrinsic optical axis, there is no limitation on the field of view.

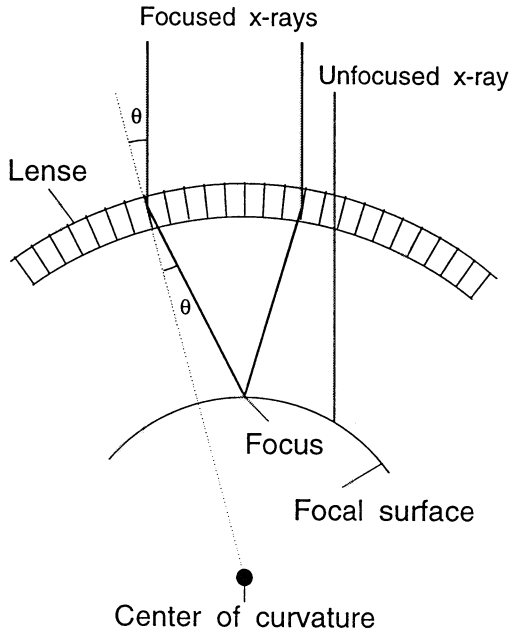

Figure 1. Geometry of a lobster eye lens.

In the x-ray range, the angular resolution of the lobster eye lens is limited primarily by geometric optics. The image on the focal cylinder will have an angular size $\Delta\theta = w/f$; where w is the channel width and f is the focal length. To obtain good angular resolution with a moderately sized telescope, it is advantageous to have pores which are as narrow as possible. For example, a 30 arcsecond image size for a 2 meter focal length requires a channel width less than 300 μm.

To efficiently reflect x-rays, the aspect ratio of the channels (the ratio of the length of the reflecting surface to the separation between reflecting surfaces) must be matched to the critical angle of reflection (Angel 1979). The most efficient lenses are those in which the channel aspect ratio is approximately equal to the inverse of the critical angle for x-ray reflection. In this case, an x-ray will typically undergo one reflection (in each plane) when traversing the lens. The optimal aspect ratio is 40:1 for 2 keV x-rays on gold and 200:1 for 15 keV x-rays on iridium.

The angular resolution of the lens is also affected by spherical aberration and diffraction. Spherical aberration depends on the range of allowed reflection angles, which is limited either by the opening angle of the pore or by the critical angle. For a channel aspect ratio of 40:1, the

maximum spherical aberration is 3 arcseconds. For reflection off gold, the aberration is less than 1 arcsecond for energies above 2.4 keV. With a pore size of 50 μm, diffraction will limit the angular resolution to 1 arcminute at 0.1 keV and 5 arcseconds at 1 keV.

In summary, a lobster eye telescope suitable for x-ray astronomy consists of a large number of small flat reflecting surfaces. For efficient x-ray reflection, the channels must have an aspect ratio matched to the critical angle of reflection and the surfaces must be smooth. To provide high resolution focusing, the surfaces must be accurately aligned and closely packed (separations on the order of 100 μm).

3 Scientific Motivation

Lobster eye optics makes possible the design of telescopes which are qualitatively different from any existing x-ray telescopes. The main new feature is the possibility of extremely large fields of view. In this section, we present sketches of two missions which would be possible with microfabricated lobster eye optics.

3.1 X-Ray Survey Telescope

The large scale structure of the universe is one of the dominant issues in contemporary astrophysics. Recent optical red shift surveys have shown the existence of structures on scales as large as the depth of the survey. Inhomogeneities on such scales are difficult to reconcile with the small amplitude of fluctuations in the microwave background detected by the Cosmic Background Explorer (Smoot 1992). The x-ray emission from clusters of galaxies can be used to trace the large scale structure and its evolution (Bahcall 1983). An x-ray survey of clusters of galaxies over a contiguous region of a few thousand square degrees of sky would provide key insights into the formation of the large scale structure and the dynamical evolution of clusters of galaxies, particularly if the observations are sensitive up to 7 keV (Sarazin 1988).

The main advantage of a lobster eye telescope in performing large surveys is its large field of view. The efficiency of a telescope for surveys is the product of the effective area and the field of view. The fields of view of conventional x-ray telescope designs are limited to one or two square degrees (Burg 1990). The field of view of a lobster eye telescope is limited only by the size and weight available on the spacecraft. We have made a concept design of a lobster eye telescope with a 2 meter focal length and a 15° by 15° field of view. The telescope and a large area proportional counter detector fit within a volume of 280 cm by 60 cm by 60 cm. This is sufficiently compact for launch as a moderate sized mission or possibly as a Small Explorer.

The telescope was designed to be sensitive up to 7 keV. The effective area is 12 cm^2 for the point focus and 26 cm^2 for all (point and line) focused x-rays at 7 keV. At 1 keV, the effective area is 27 cm^2 for the point focus and 92 cm^2 for all focused x-rays. This is substantially less than for a Wolter telescope of the same focal length. However, for survey work the vast increase in field of view more than compensates for the reduced effective area. If we calculate the product of point focus effective area times field of view for the lobster eye telescope, we find 2400 $cm^2 degree^2$ at 7 keV and 5400 $cm^2 degree^2$ at 1 keV. This is an order of magnitude improvement in survey efficiency compared with a Wolter telescope designed for a survey mission (Burg 1990).

3.2 Hard X-Ray Telescope

Imaging x-ray telescopes that are efficient at energies between 10 and 40 keV would provide an abundant scientific return (Elvis 1987). Potential scientific results include unambiguous identification of cyclotron lines from neutron stars, which would allow determination of the magnetic field strength and geometry; measurement of the temperature and spectra of gas in clusters of galaxies, providing important information on galaxy formation and clustering; and measurement of weak point source spectra near 35 keV, which could resolve the question of the origin of the x-ray background. A mission to perform hard x-ray imaging and spectroscopy was given the highest priority of all future missions by the high energy astrophysics panel of the Bahcall committee (Margon 1991).

Current concepts for hard x-ray imaging include large area coded aperture mask telescopes, Kumakov concentrators, and Kirkpatrick-Baez telescopes. Coded aperture telescopes have higher background than focusing devices, since the photons from each source are scattered across half the detector plane. Good sensitivity is possible with coded aperture telescopes only if the telescope and detector are very large. Spectral measurement of weak sources will probably require focusing optics.

Perhaps the leading candidate for hard x-ray focusing optics are long focal length Kirkpatrick-Baez telescopes. A prototype telescope constructed by Joy and Weisskopf (1991) of 0.72 mm thick silicon wafers has a focal length of 15.8 meters. The most expensive part of such a telescope is likely to be the structure joining the lens with the detector and the active control system required to maintain the alignment (Weisskopf 1991). Using microstructures, the same energy band pass and effective area could be achieved using sixteen telescopes with 4-m focal length. The microstructure telescope array would have the disadvantage of requiring sixteen detectors, albeit with the same total detection area. However, the short focal length of the telescopes would not require a complex support structure. A mission based on microfabricated telescopes would have a lower total cost than the equivalent long focal length design and have an inherent high level of redundancy.

Another candidate for hard x-ray focusing optics are Kumakov concentrators. These devices consist of a large number of optic fibers bent so that parallel light rays entering the device are concentrated on a small spot at the exit. The x-rays undergo multiple reflections in the fibers. To obtain efficient concentration at high energies, it is necessary to use grazing angles of a fraction of an arcminute. Only x-rays within this narrow cone of angles are concentrated; therefore, the pointing of the telescope must be maintained to an accuracy of a few arcseconds throughout an observation.

The lobster eye design has a critical advantage in this regard. Lobster eye telescopes have no optical axis and therefore do not suffer from a degradation of effective area off axis. While the spacecraft pointing must be accurately measured, precise active control is not required. In fact, if the field of view of the telescope is large enough to contain a few bright sources and the drift rate of the spacecraft is small, the lobster eye can determine its own pointing and a high accuracy optical tracker is not required. Easing the pointing requirements should greatly reduce the cost of a pointing system for a high energy lobster mission.

4 Results

4.1 MCP Lenses

Lobster eye x-ray optics were first fabricated using glass microchannel plate (MCP) technology. MCP's were first used to focus x-rays by Wilkins (1987). Our group was the first to use square pore MCP's, which have a vastly higher focusing efficiency than standard circular pore plates. Our results have been published in Applied Optics (Kaaret 1992). The reader is referred to that paper for a detailed description. Our main results are summarized briefly below.

The surfaces of individual MCP channels were measured and found to have high microroughness transverse to the channel axis and low microroughness parallel to the axis. A total of six measurements were made on the three types of MCP's of which we had samples: hydrogen reduced MCP's from Philips, hydrogen reduced MCP's from Galileo, and unreduced MCP's from Galileo. The roughness on all the MCP's has the same form, grooves that run along the length of the MCP pores. The values of the roughness vary from plate to plate. The best values are for the hydrogen reduced Galileo MCP. For this MCP, the high frequency transverse roughness has an RMS value of 5.9 nm and a gaussian autocorrelation function with correlation length 1.41 μm. The roughness is significantly worse than the 1.5 nm typical for metal foil optics (Christensen 1991). These longitudinal grooves form a random grating in the conical diffraction geometry. The parameters of the grating can be derived from the surface profile measurements. With the addition of conical diffraction using the measured surface parameters to our ray tracing code, we were able to accurately reproduce the x-ray images observed.

The best results on the angular alignment of MCP pore surfaces come from G. Fraser of the University of Leicester, England. Fraser and collaborators observed the cruciform image structure of a two dimensionally focusing MCP lens in the soft x-ray band (Fraser 1992). They used a second generation MCP made by Galileo Electro-Optics. During the manufacture of this MCP, special procedures were used to ensure good alignment of the pore surfaces. The MCP represents the best available technology in MCP manufacture. Fraser *et al.* illuminated the entire surface of the MCP with silicon K-α radiation (1.74 keV) and observed the image produced. They measured an angular resolution of 5.05 x 15.1 arcminutes FWHM along the two perpendicular axes (Fraser 1993). These results are far better than what we obtained with first generation MCP's. However, they are significantly worse than the 2 arcminute resolution that can be obtained with metal foil optics (Christensen 1991).

Our tests of MCP optics proved the concept of lobster eye optics in the x-ray regime. Our measurements, together with those of Fraser, have shown the limitations of the MCP fabrication technique. We conclude that neither the first nor the second generation square MCP's are adequate for use in x-ray astronomy. Development of suitable MCP optics will require improvements in the MCP manufacturing process.

4.2 Silicon Lenses

The limitations of MCP optics led us to consider new techniques for the fabrication of lobster eye optics. Replication of identical rectilinear micron scale structures is common procedure in the microelectronics industry. Techniques exist for the manufacture of microstructures which have crystal planes as surfaces. The crystal planes of a single crystal are extremely flat and accurately aligned; they seem to be ideal optical surfaces. These techniques are promising for

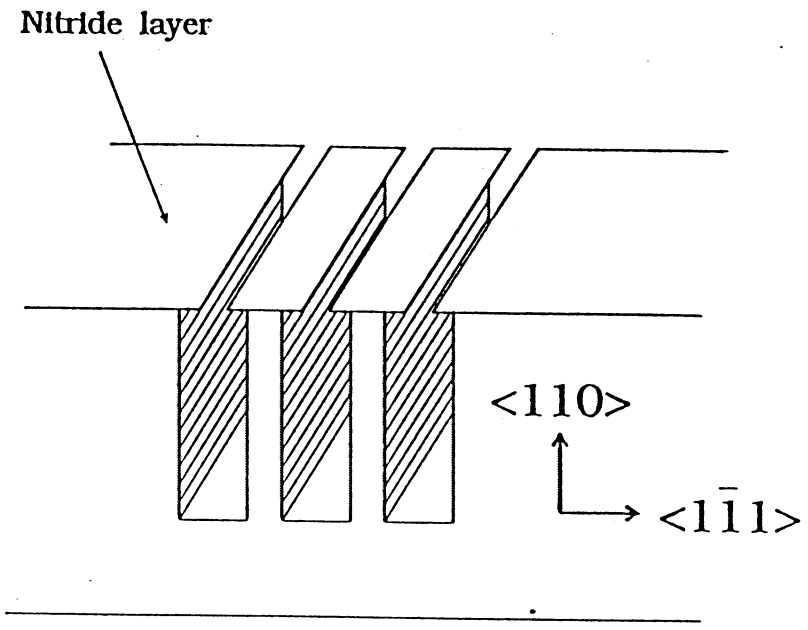

Figure 2: Geometry of anisotropic etching.

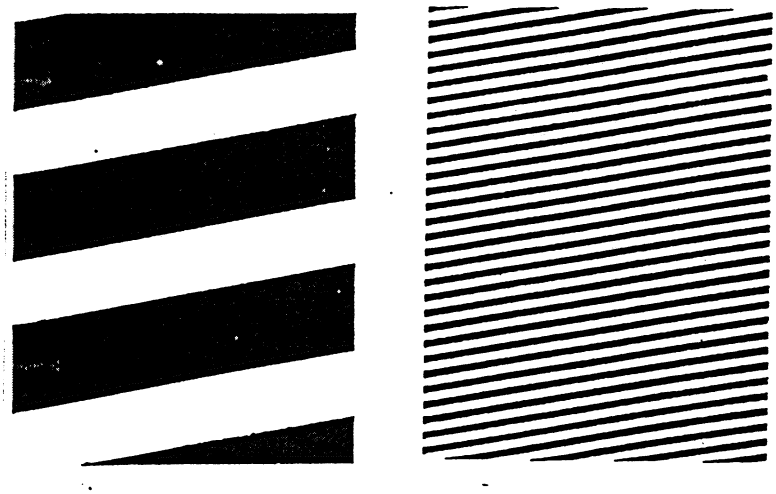

Figure 3: Photograph of the front surface of an etched wafer.

the manufacture of lobster eye optics. They permit the fabrication of the required structures in a geometry with inherently good alignment.

Silicon crystals are commonly used by solid state physicists and electrical engineers as x-ray mirrors because of the extremely good surface quality of a highly polished wafer. One-dimensionally focusing mirrors have been constructed by bending thin wafers into a cylinder (Kaminsky 1987). However, these laboratory optics do not have the large area required for astronomical applications. The application of silicon to astronomical x-ray optics has been pioneered by Joy and Weisskopf (1991). As a first step, they measured the surface of a sample wafer using an optical profilometer. On spatial scales less than 0.1 mm the silicon surface met or surpassed the AXAF mirror requirements. However, significant surface errors were found on scales greater than a few millimeters. These errors seem to arise from bending the wafers. While the mid-scale surface errors are a significant problem for the large telescope (15.8 meter focal length) constructed by Joy and Marshall, they should not be a problem if the optical surfaces are shorter than a few millimeters, as will be the case in our lobster eye lenses.

An array of parallel reflecting surfaces can be constructed by etching pores completely through a silicon wafer. A 2-d lobster eye telescope consists of square pores in a spherical geometry and a 1-d lobster eye consists of rectangular pores in a cylindrical geometry. Due to the problems involved in bending a silicon wafer into a spherical shape, we plan to concentrate initially on the construction of 1-d silicon lobster eye lenses. Lenses that focus in two dimensions can be obtained by crossing two 1-d focusing lenses (similar to a KirkPatrick-Baez geometry).

4.2.1 Fabrication

We fabricate lobster eye lenses by anisotropically etching rectangular pores completely through a single crystal silicon wafer. Single crystal silicon has a diamond cubic lattice, the most closely packed lattice in which each atom has four nearest neighbors. The nearest neighbor distance is 2.43 Å while the lattice spacing is 5.43 Å. In a cubic lattice, crystal directions are perpendicular to their corresponding crystal planes. The crystal planes most often referred to are the <100>, <110>, and <111> planes. Anisotropic etching uses a chemical which etches certain silicon crystals planes more rapidly than others. The best available anisotropic etchant etches <100> and <110> silicon planes as much as 500 times faster than <111> planes (Kendall 1975). The geometry of anisotropic etching is shown in Figure 2. By aligning the <111> planes perpendicular to the wafer surface, it is possible to etch a pattern completely through a wafer with very little distortion. We etched rectangular pores completely through <110> oriented silicon wafers. The larger surfaces of the pores (the mirror elements) were aligned with the <111> planes of the crystal.

The crucial steps in etching a wafer are:
1) Depositing a mask of a material that will not be etched.
2) Exposing a photolithographic pattern, aligned with the crystal structure, onto the lens.
3) Removing the exposed areas of the masking layer.
4) Performing the etch.
5) Removing the mask and cleaning the wafer.

The Micro Devices Laboratory (MDL) at JPL has an active program for the development of silicon micromachining techniques for space applications. Our research program fit well into the

overall MDL program goals as it required the development of new techniques in order to meet new scientifically motivated requirements. The first fabrication was done by Dr. Kenny during the spring of 1992. Subsequent fabrication was done by Mr. Chen under the supervision of Dr. Kenny during the summers of 1992 and 1993.

4.2.2 First Lenses

The first set of lenses was fabricated as a proof of concept that silicon micromachining could be used to produce relatively large (millimeter deep) structures that were accurately aligned. We selected potassium hydroxide (KOH) as the anisotropic etch because it has the highest selectivity of any anisotropic etch. The initial etch solution was 44g KOH:100mL H_2O at 50°C. Ideally, this solution will have a <110>/<111> etch rate ratio of 400:1. In practice this ratio is reduced due to mask misalignment, surface contamination and defects, and the difficulty of refreshing the solution deep in the etched grooves. Nevertheless, we have achieved etch ratios of better than 100:1.

KOH also etches SiO_2, the most convenient masking film. Since the rate at which KOH etches oxide is approximately the same as its etch rate on the <111> plane of silicon, we first tried to use a thick (3 μm) oxide as our masking layer. Unfortunately, this caused severe stress on the crystal structure of the substrate, resulting in drastic and uneven undercutting. Furthermore, the damage to the crystal remained even after the oxide was stripped off by HF, rendering those wafers useless for our experiments. We were forced to abandon oxide and use a Si_3N_4 layer instead. The disadvantage of using a nitride layer is that unlike oxygen, nitrogen does not diffuse significantly through silicon. The nitride layer must be deposited by chemical vapor deposition (CVD). We tried several different nitride deposition systems at JPL, Caltech, and Berkeley. The only one that achieved acceptable results was the low pressure CVD system at Berkeley. Their process deposits a nitride layer with a higher than normal silicon content to reduce the stress resulting from thermal expansion and contraction during deposition. The result is a nitride layer that is exceptionally sturdy and free of pinholes. The Microdevices Laboratory at JPL is currently acquiring the same system for in-house nitride deposition.

We started with 2" diameter, <110> oriented single crystal silicon wafers with thicknesses ranging from 800 to 2000 μm. A 0.5 μm silicon nitride layer was deposited on both sides of the wafer. Each silicon crystal is cut with a "flat", a surface which is nominally aligned with the crystal planes. Typically, the flat is parallel with the <111> planes perpendicular to the surface to an accuracy of 1°. We used the flat to align a photolithographic mask, consisting of 15 μm wide rectangular channels on 100 μm centers. The exposed nitride was removed using a CF_4 plasma reactive ion etch (RIE). After stripping the photoresist, the wafer was placed in a quartz etching apparatus containing the KOH solution, which was periodically manually refreshed to maintain the correct concentration and remove dissolved silicon. The wafer took more than thirty days to etch through completely, after which the remaining nitride was removed by a phosphoric acid etch. Due to undercutting, the resulting channels were approximately 50 μm wide.

A photograph of one of our first lenses is shown in Figure 3. The lens is 800 μm thick and has 50 μm wide channels and a 100 μm period. The wafer is 2 inches in diameter and the lens has a projected surface area of approximately 10 cm^2. Our first silicon lenses show alignment vastly superior to the best MCP lenses. Because the channels are etched along the crystal planes

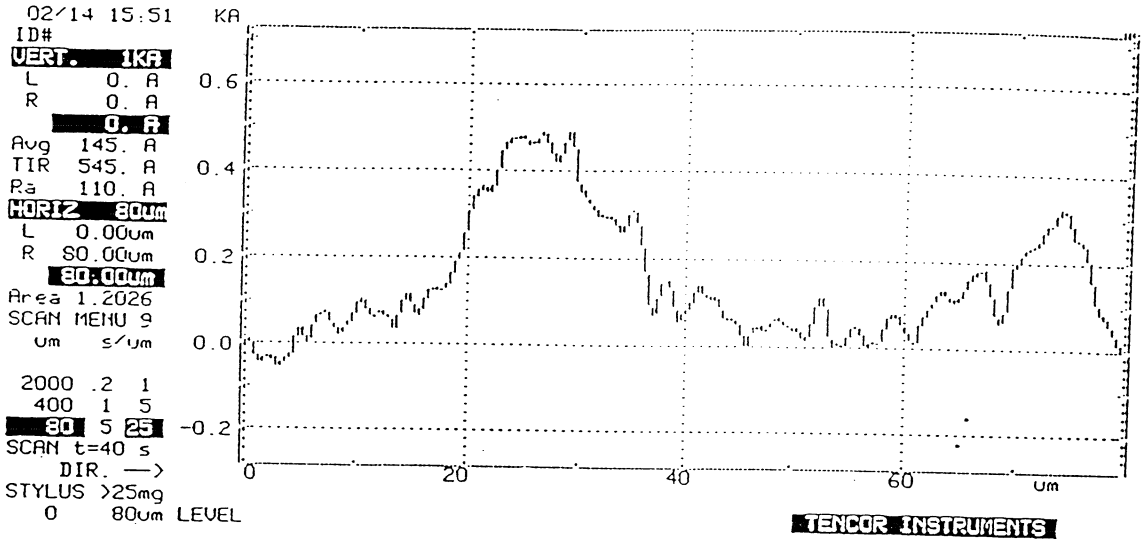

Figure 4: Surface profile of the etched <111> surface from the first set of lenses.

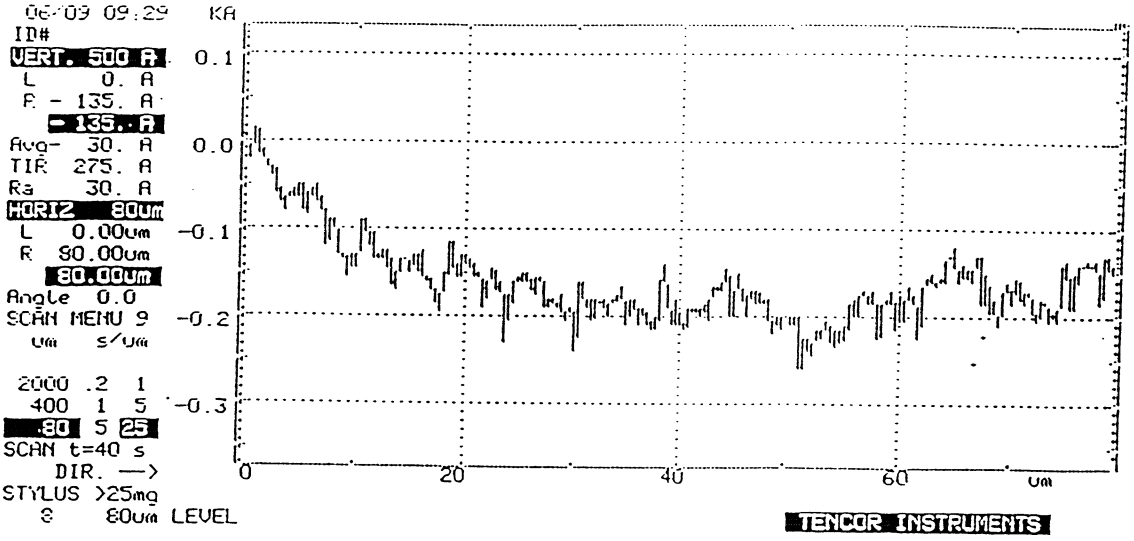

Figure 5: Surface profile of the etched <111> surface from the second set of lenses.

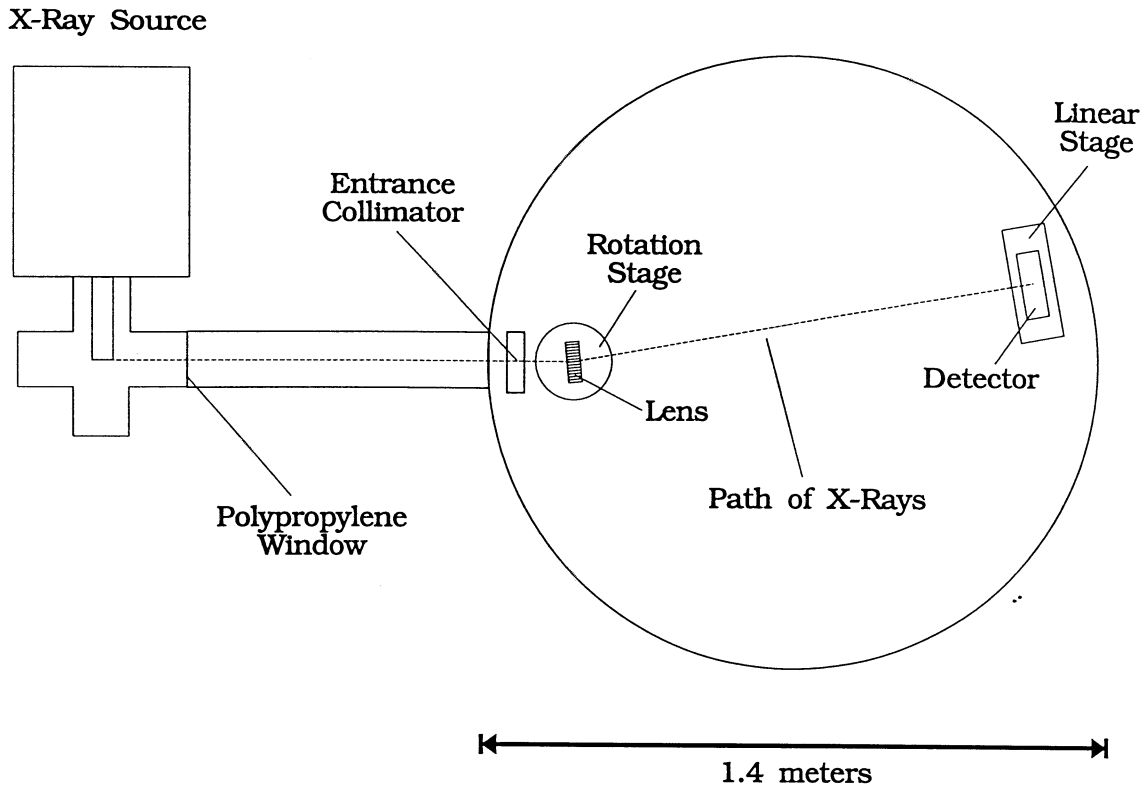

Figure 6: X-ray beam line for tests of microfabricated lenses.

of the silicon lattice, the reflecting walls that are produced show excellent alignment. We consider the channel-to-channel alignment problem to be completely solved with this technique.

We measured the surface profile of the anisotropically etched reflecting planes of a 2000 μm thick lens using a Tencor Alpha-Step stylus profilometer. The surface profile from a representative section of the <111> surface is shown in Figure 4. The surface roughness is approximately 110 Å RMS over small regions. Roughness of this magnitude would produce significant image degradation due to scattering. We concluded that the reactive ion etch (RIE) that removes the remaining nitride layer after the KOH etch may be the source of the roughness.

4.2.3 Second Lenses

For the second series of lenses a number of improvements were made in the fabrication procedure. The mask deposition technique was not altered, as the silicon nitride mask had been proven to perform well.

To improve the alignment of the photolithographic pattern, we used the anisotropic etch to find the true crystal plane orientation before aligning the lens pattern. After depositing the mask, we expose a "wagon wheel" pattern onto a small region of the wafer. The pattern consists of a number of lines, all pointed towards a common origin, rotated through small fractions of a degree

relative to each other. We expose this pattern and perform a shallow etch; the lines most closely aligned with the crystal planes survive the etch. This technique allows us to determine the alignment of the crystal planes to 0.1° accuracy, instead of the 1° degree accuracy of the manufacturer's alignment flat.

To improve the etch process, a wafer agitator was designed by Nashrid Kibria, an undergraduate at Columbia. A suitable agitator was not commercially available. The agitator is used to refresh the solution more thoroughly in the very deep grooves of thick wafers to improve the etch rate and etch selectivity. It was also decided to reduce the temperature of the etch to room temperature and increase the concentration to 44%wt KOH in H_2O. According to the literature, KOH is more selective at lower temperatures, although the overall etch rate is also reduced. Finally, the nitride layer remaining after etching was removed using phosphoric acid, a chemical etch, instead of by RIE.

Using a process incorporating these improvements, we produced 1 mm thick wafers with 15 μm pores spaced 100 μm apart. The undercutting has been drastically reduced to approximately 5 μm for the entire 1 mm depth, making the channel aspect ratio 40:1. We performed measurements of the <111> etched surfaces of these newer wafers. The surface profile from a representative section of the <111> surface is shown in Figure 5. The RMS roughness is on the order of 30 Å, compared to 110 Å for our first wafers. However, the surface still exhibits large step features.

4.3 X-Ray Test Facility

During the summer of 1993, Eric Ford, a graduate student at Columbia, and Jay Demas, an undergraduate at Columbia, constructed a facility that allows us to test the x-ray reflectivity of our lenses at angles up to 15°, as well as perform Bragg scattering measurements at angles up to 50° (see Figure 6). A water-cooled x-ray source built at Columbia is housed in a small vacuum chamber with a polypropylene x-ray window. X-rays pass through a 1 meter pipe into a large steel chamber containing an optical table. On the optical table are mounted an entrance collimator, a lens holder on a rotating stage, and a non-imaging proportional counter on a linear stage. The detector has a narrow (adjustable) entrance aperture. The one-dimensional intensity profile is reconstructed by scanning the detector along the range of the linear stage. The linear stage can be attached to a number of positions on the table, each 1 meter away from the lens. By choosing an appropriate position and adjusting the micropositioners on the rotating and linear stages, any θ-2θ combination up to a maximum of $\pm 15°$ can be achieved. The detector can also be mounted at positions that are 0.5 m away from the lens at wider angles selected for Bragg scattering measurements on silicon. The x-ray source can accept a number of different anodes to generate characteristic x-rays lines up to 6 keV. The main chamber is pumped down to 10^{-3} torr by a mechanical pump, while an ionization pump brings the source chamber below 10^{-6} torr. Using this chamber it is possible to make measurements on our lenses with x-rays in an energy range extending from the carbon K line (277 eV) to the iron K line (6.4 keV).

5 Conclusion

Lobster eye optics are a novel x-ray optical technique which may allow the construction of future scientifically productive x-ray astronomy missions with low total mission costs. The goal of this research program was to fabricate a prototype x-ray lens with 100-micron-scale optical elements using anisotropic etching of single crystal silicon wafers. Requirements on the geometry, surface alignment, and surface quality of the lens were determined by considering the scientific goals of future x-ray astronomy missions. We have established that micromachined lenses can be made with the proper geometry and alignment accuracy (Chen 1993, 1994). We made significant progress towards solving the remaining problem of surface roughness, obtaining an RMS roughness of 30 Å in our most recent wafers.

6 References

J.R.P. Angel, *Astrophys. J.* **233,** 364 (1979).

A. Chen, P. Kaaret, and T. Kenny, *Proc. SPIE*, **2279**, 298 (1994)

A. Chen, P. Kaaret, and T. Kenny, *Proc. SPIE*, **2011**, 227 (1993)

F.E. Christensen *et al., Proc. SPIE* **1546**, 53 (1991)

M. Elvis, D.G. Fabricant, and P. Gorenstein, *Applied Optics* **27**, 1481-1485 (1988).

G.W. Fraser *et al.*, *Nucl. Inst. Meth.* **A324**, 404-407 (1993); orig. *Proc. SPIE* **1546** (1992).

G.W. Fraser *et al.*, to appear in *Proc. SPIE* **2011** (1993).

P. Gorenstein, *Proc. SPIE* **1741** (1992).

R.W. Hardeman *et al.*, *Surf. Sci.* **152/153**, 1051 (1985).

M.K. Joy, and M.C. Weisskopf, *Proc. SPIE* **1546,** 303 (1991).

P. Kaaret and P. Geissbühler, *Proc. SPIE* **1546,** 82 (1991).

P. Kaaret *et al.*, *Applied Optics* **31**, 7339-43 (1992).

D.L. Kendall, *Appl. Phys. Lett.* **26**, 195 (1975).

D.L. Kendall, *Ann. Rev. Mat. Sci.* **9**, 373 (1978).

D.L. Kendall, *J. Vac. Sci. Technol.* **A8**, 3598-3604 (1990).

M.A. Kumakhov, *Nucl. Inst. Meth.* **B48**, 283-286 (1990).

M.A. Kumakhov and F.F. Komarov, *Phys. Reports* **191**, 289-350 (1990).

T.W. Kenny, in Microtechnologies and Applications to Space Systems, JPL Workshop (1992).

S.M. Lea, R. Mushotzky, and S. Holt, *Astrophys. J.* **262,** 24 (1982).

Y. Namba and H. Tsuwa, *Annals of CIRP* **27**, 511 (1978).

E.D. Palik, V.M. Bermudez, and D.J. Edell, *J. Electrochem. Soc.* **132**, 871 (1985).

K.E. Petersen, *Proc. IEEE* **70**, 420 (1982).

G. F. Smoot *et al.*, *Ap. J. Lett.* **396**, L1-5 (1992).

S.W. Wilkins, *et al, Rev. Sci. Instrum.* **60,** 1026 (1989).